



A Facile One Pot Synthesis and Anticorrosion Potential of Carbazole Linked Quinoline Moiety

V. PANNEERSELVI¹, P. MUTHUKRISHNAN², K. SHANKAR³ and K. PRABAKARAN^{1,*}

¹Department of Chemistry, P.S.G. College of Arts & Science, Coimbatore-641014, India

²Department of Chemistry, SRM TRP Engineering College, Tiruchirappalli-621105, India

³Department of Chemistry, Government College of Technology, Coimbatore-641013, India

*Corresponding author: E-mail: prabakaranchem@gmail.com

Received: 12 November 2023;

Accepted: 15 December 2023;

Published online: 31 December 2023;

AJC-21508

A facile and efficient one pot synthesis has been developed for the preparation of quinoline-substituted carbazoles 3-(4-carboxyquinolin-2-yl)-9-methyl-9H-carbazole (**Cbz-QCA**) and 3-(4-chloroquinolin-2-yl)-9-methyl-9H-carbazole (**Cbz-CIQ**) by treating 3-acetyl-9-methyl-9H-carbazole (**3Ac-Cbz**), with isatin under Pfitzinger reaction conditions and utilizing anthranilic acid in the presence of POCl₃ through the modified Niementowski method, respectively. The synthesized compounds have been comprehensively characterized through spectral data. The effect of **3Ac-Cbz** (**1**), **Cbz-QCA** (**2**) and **Cbz-CIQ** (**3**) were assessed as a steel corrosion inhibitor in 1M HCl using weight loss, potentiodynamic polarization and electrochemical methods. The inhibitory effect increases with the synthesized inhibitor concentration, reaching above 84% at higher concentrations of all tested inhibitors. These results indicated that synthesized inhibitors have a good corrosion inhibition. An increase in the concentration of inhibitor leads to a higher percentage of inhibition efficiency, driven by the adsorption of inhibitor molecules onto the metal surface. The scanning electron microscope (SEM) images confirmed the successful outcomes of the experimental inhibitory tests and validate the adsorption process.

Keywords: Carbazole derivatives, Quinoline derivatives, Pfitzinger reaction, Niementowski reaction, Electrochemical corrosion.

INTRODUCTION

Carbazoles and quinolines are the significant nitrogen-containing heterocyclic compounds display a diverse array of biological functions such as antioxidants, analgesics, antidiabetic and anti-inflammatory properties [1,2]. These nitrogen heterocyclic compounds have shown significant importance and known to be extracted from a plant family called rutaceae, which is predominantly found in southeast Asia [1]. The carbazoles exhibit remarkable ease of sourcing from nature and feature straightforward synthetic pathways, making them quite fascinating [3]. Among the various heterocyclic compounds, carbazole linked quinoline with appropriate substituents are important candidates capable of fulfilling key criteria for efficient corrosion control inhibitors, because of their chemical composition, comprising heteroatoms and π -electrons in a delocalized arrangement [4,5]. These are known to be principal elements of heterocyclic mixtures that could join different useful gatherings, for example, amino, methoxy, hydroxyl and carboxylic groups

coexist within a single molecule, exhibiting an affinity for metal surfaces [6,7].

Organic corrosion inhibitors have certain aromatic rings, with a high electron density and a number of heteroatoms (O, N, P and S) that encourage their adsorption across the complete metal surface, thereby slowing the process of corrosion [8]. The presence of electronegative functional groups, electrons engaged in triple or conjugated double bonds and the existence of heteroatoms like O, N, P and S in the organic compound structure are all important considerations when selecting an effective inhibitor for metal corrosion, agreeing to Wang *et al.* [9]. These locations have been learnt to provide incomparable adsorption sites [9-13]. However, based on current knowledge, there are limited instances where the carbazole structure is substituted with a quinolone unit. Consequently, the synthesis of such compounds is sought after for inhibition of metal corrosion in acidic environment.

Most of the reports conclude that the compounds azole, azine and pyridine [14,15] remain efficient corrosion inhibitors

up to 80 °C. The syntheses of novel organic molecules result in a variety of molecular configurations with several heteroatoms and substituents. The development of an adsorptive coating with a physical or chemical composition set on the metal exterior is the typical explanation for their adsorption [16-18]. Due to the positive results obtained from pyrazolic compounds, we intended to synthesize more compounds and evaluate their effect on the corrosion resistance of steel in acidic conditions [19,20]. Acetylcarbazole (**1**) was used as the useful synthon for the synthesis of various substituted carbazole heterocycles. Hence, this study introduces the synthesis and inhibitive effects of 3-acetyl-9-methyl-9*H*-carbazole (**3Ac-Cbz**), 3-(4-carboxyquinolin-2-yl)-9-methyl-9*H*-carbazole (**Cbz-QCA**) and 3-(4-chloroquinolin-2-yl)-9-methyl-9*H*-carbazole (**Cbz-ClQ**), functioning on corrosion of mild steel in 1 M HCl. The selection of **3Ac-Cbz** (**1**), **Cbz-QCA** (**2**) and **Cbz-ClQ** (**3**) as corrosion inhibitors in this study aims to investigate their potential as aqueous corrosion, as well as to comprehend the interactions involving carbazoles interact with the surface of mild steel.

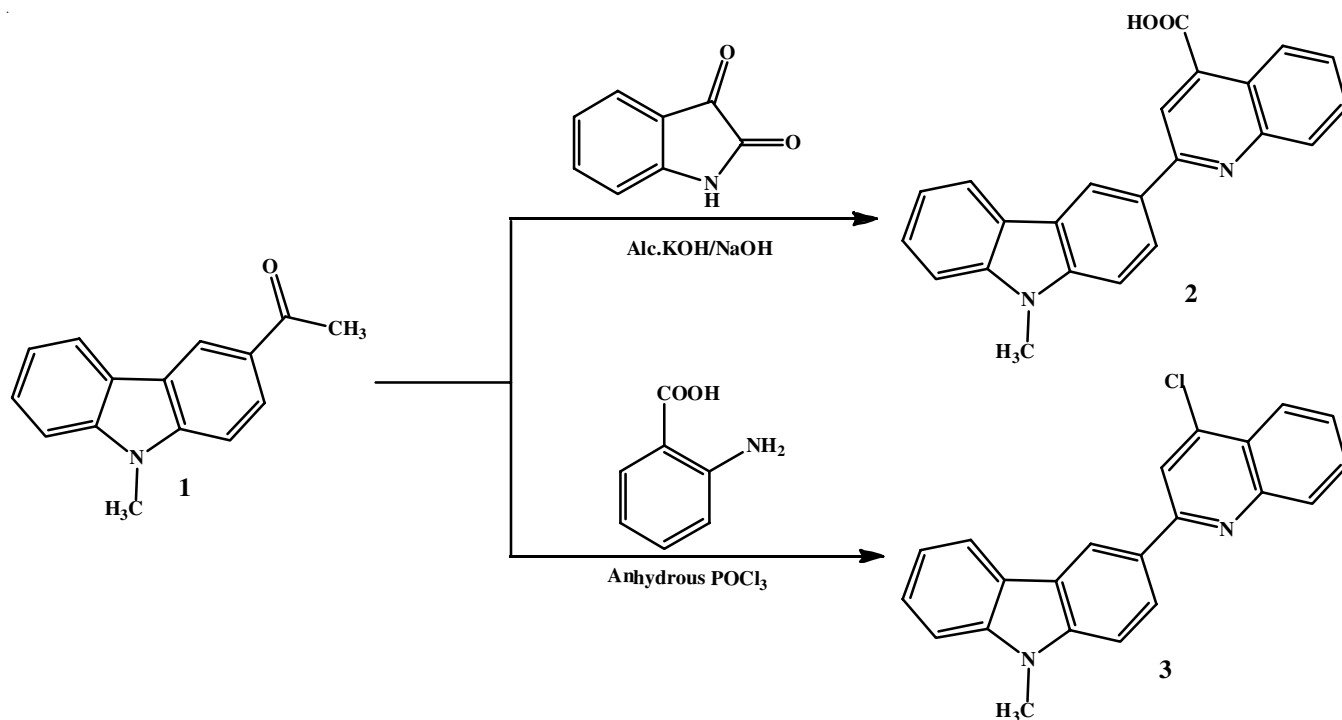
EXPERIMENTAL

All the chemicals were purchased from Rankem and Merck and employed in this work without additional purification. The melting points were determined using a Mettler FP 51 apparatus (Mettler Instruments, Switzerland) and are uncorrected. The FT-IR spectra were recorded using Shimadzu FT-IR spectrophotometer in the range of 4000-400 cm^{-1} . The ^1H & ^{13}C NMR spectra were recorded on a Varian-400 MHz (^1H) and 100 MHz (^{13}C) spectrometers, respectively using CDCl_3 and $\text{DMSO-}d_6$ as solvents. The mass spectra were taken on Agilent single quad mass spectrometer. Compound 3-acetyl-9-methyl-9*H*-carbazole (**3Ac-Cbz**, **1**) was synthesized according to reported procedure

[21-23]. Product purity was assessed through TLC plates coated with silica gel-G, employing a mixture of petroleum ether and ethyl acetate as mobile phase.

Synthesis of 3-(4-carboxyquinolin-2-yl)-9-methyl-9*H*-carbazole (Cbz-QCA, **2):** A mixture of 3-acetyl-9-methyl-9*H*-carbazole (0.5 g, 1 mmol), isatin (0.3 g, 1 mmol) and NaOH (2 mmol, 0.27 g) in ethanol was subjected to reflux using a steam bath for 24 h. The progression of the reaction was examined by TLC. Following completion of the reaction, the excess solvent was removed and the resulting solution was added to ice and neutralized using dil. HCl. The obtained crude solid was filtered and subjected to purification through the treatment with Na_2CO_3 , followed by neutralization using dil. HCl. By recrystallizing the solid from ethanol, corresponding 3-(4-carboxyquinolin-2-yl)-9-methyl-9*H*-carbazole (**2**) was obtained (**Scheme-I**). Yield: 81%, brown solid, m.p.: 210 °C, IR (KBr, ν_{max} , cm^{-1}): 1056, 1596, 1627, 2400-3400. ^1H NMR (400 MHz, CDCl_3 , δ ppm): 3.94, (s, 3H, $\text{N}_9\text{-CH}_3$), 7.26 (t, 1H, $J = 7.2\text{Hz}$), 7.49-7.58 (m, 2H), 7.64 (d, 1H, $J = 8\text{ Hz}$), 7.39-7.78 (m, 2H), 8.10 (d, 1H, $J = 8.4\text{ Hz}$), 8.37 (d, 1H, $J = 7.6\text{ Hz}$), 8.43 (s, 1H), 8.47 (d, 1H, $J = 10.5\text{ Hz}$), 8.63 (d, 1H, $J = 9.2\text{ Hz}$), 9.10 (s, 1H). ^{13}C NMR (100 MHz, CDCl_3 , δ ppm): 29.19, 109.47, 119.28, 119.35, 120.70, 122.40, 122.46, 123.14, 125.15, 125.97, 126.07, 126.51, 129.14, 129.44, 141.23, 141.57, 148.42, 156.55, 186.23. MS: (calcd. 352), m/z ($[\text{M}+\text{H}]^+$): 353; Anal. calcd. (found) % for $\text{C}_{23}\text{H}_{16}\text{N}_2\text{O}_2$: C, 78.36 (78.32); H, 4.55 (4.57); N, 7.92 (7.95).

Synthesis of 3-(4-chloroquinolin-2-yl)-9-methyl-9*H*-carbazole (Cbz-ClQ) (3**):** A mixture of 3-acetyl-9-methyl-9*H*-carbazole (0.5 g, 1 mmol), anthranilic acid (0.123 g, 1 mmol) in 5 mL of POCl_3 was subjected to reflux at 120 °C for 3 h. The progression of the reaction was examined by TLC. Once the reaction was finished, the mixture was poured into ice water



Scheme-I: Synthesis of Cbz-QCA (**2**) and Cbz-ClQ (**3**)

and stirred continuously. It was then subjected to extraction using ethyl acetate. The crude product attained in this manner was further refined through column chromatography using a silica gel column and eluting with a mixture of petroleum ether and ethyl acetate (99:1). This process yields the corresponding 3-(4-chloroquinolin-2-yl)-9-methyl-9*H*-carbazole (**3**) (**Scheme-I**). Yield: 89%, white solid, m.p.: 180 °C. IR (KBr, ν_{\max} , cm^{-1}): 1249, 748, 1141, 1481, 1581, 2924, 3464. $^1\text{H NMR}$ (400 MHz, CDCl_3 , δ ppm): 3.94, (s, 3H, $\text{N}_9\text{-CH}_3$), 7.29-7.36(m, 1H), 7.47 (d, 1H, $J = 8$ Hz), 7.54-7.58 (m, 2H), 7.63-7.65 (dt, 1H, $J = 4, 8$ Hz), 7.82 (dt, 1H, $J = 4, 8$ Hz), 8.16 (s, 1H), 8.24-8.28 (m, 3H), 8.37 (dd, 1H, $J = 4, 8$ Hz), 8.95 (d, 1H, $J = 4$ Hz). $^{13}\text{C NMR}$ (100 MHz, CDCl_3 , δ ppm): 29.31, 108.74, 108.78, 119.14, 119.45, 120.67, 123.12, 123.36, 123.96, 124.97, 125.40, 126.12, 126.65, 129.50, 129.74, 130.47, 141.58, 142.08, 142.90, 149.20, 158.05. MS. (calcd. 342), m/z ($[\text{M}+\text{H}]^+$): 343; Anal. calcd. (found) % for $\text{C}_{22}\text{H}_{15}\text{N}_2\text{Cl}$: C, 77.05 (77.14); H, 4.38 (4.43); N, 8.14 (8.16).

Weight loss measurements: The utilization of the weight loss approach is both desired and reliable for assessing the efficiency of corrosion inhibitors. Pre-determined quantities of mild steel samples were immersed in a test solution, both with and without different inhibitor concentrations. The inhibition efficiency (IE), corrosion rate (CR) and surface coverage (θ) and the calculations were performed using the following eqns. 1-3:

$$\text{Inhibition efficiency (\%)} = \frac{W_1 - W_2}{W_1} \times 100 \quad (1)$$

$$\text{Corrosion rate} = 534 \times \frac{W_b - W_a}{\text{DST}} \quad (2)$$

$$\text{Surface coverage (\theta)} = \frac{\text{CR}_0 - \text{CR}_1}{\text{CR}_0} \quad (3)$$

where CR_0 and CR_1 are corrosion rate of blank and inhibitor solutions, $\Delta W = (W_1 - W_2)$, here, W_1 and W_2 represent the weight loss of mild steel in the absence and presence of inhibitor, respectively and D denotes the density of mild steel (7.8 g cm^{-3}), A represents the area of the specimen in cm^2 and T represents the immersion period in hours.

Electrochemical analysis: The electrochemical measurements were conducted by employing CH electrochemical analyzer model 604D with in a standard three-electrode glass cell. The working electrode was composed of mild steel coupon with a 1 cm^2 exposed area. The counter electrode was made up of platinum and the saturated calomel electrode serves as reference electrode. Potentiodynamic polarization curves were generated by sweeping the potential at a specified rate of 1 mV s^{-1} , beginning from a cathodic potential of +300 mV and sweeping to an anodic potential of -300 mV, all related on the way to the open circuit potential. The experiments were conducted without any stirring and performed under the atmospheric conditions. Electrochemical impedance spectroscopy measurements were conducted across a frequency range spanning from $1 \times 10^5 \text{ Hz}$ to 0.1 Hz and superimposed by sine wave having an amplitude 5 mV. Subsequently, the charge transfer resistance (R_{ct}) and

double layer capacitance (C_{dl}) were determined using the obtained data from the Z' vs. Z'' plot. The IE (%) was determined using a specific formula:

$$\text{IE}_{\text{Pol}} (\%) = \frac{I_{\text{corr}} - I_{\text{corr (inh)}}}{I_{\text{corr}}} \times 100 \quad (4)$$

$$\text{IE}_{\text{EIS}} (\%) = \frac{R_{\text{ct (inh)}} - R_{\text{ct}}}{R_{\text{ct (inh)}}} \times 100 \quad (5)$$

where I_{corr} and $I_{\text{corr (inh)}}$ represent the corrosion current density without and with inhibitor, respectively. The charge transfer resistances obtained without and with the inhibitors are denoted as R_{ct} and $R_{\text{ct (inh)}}$.

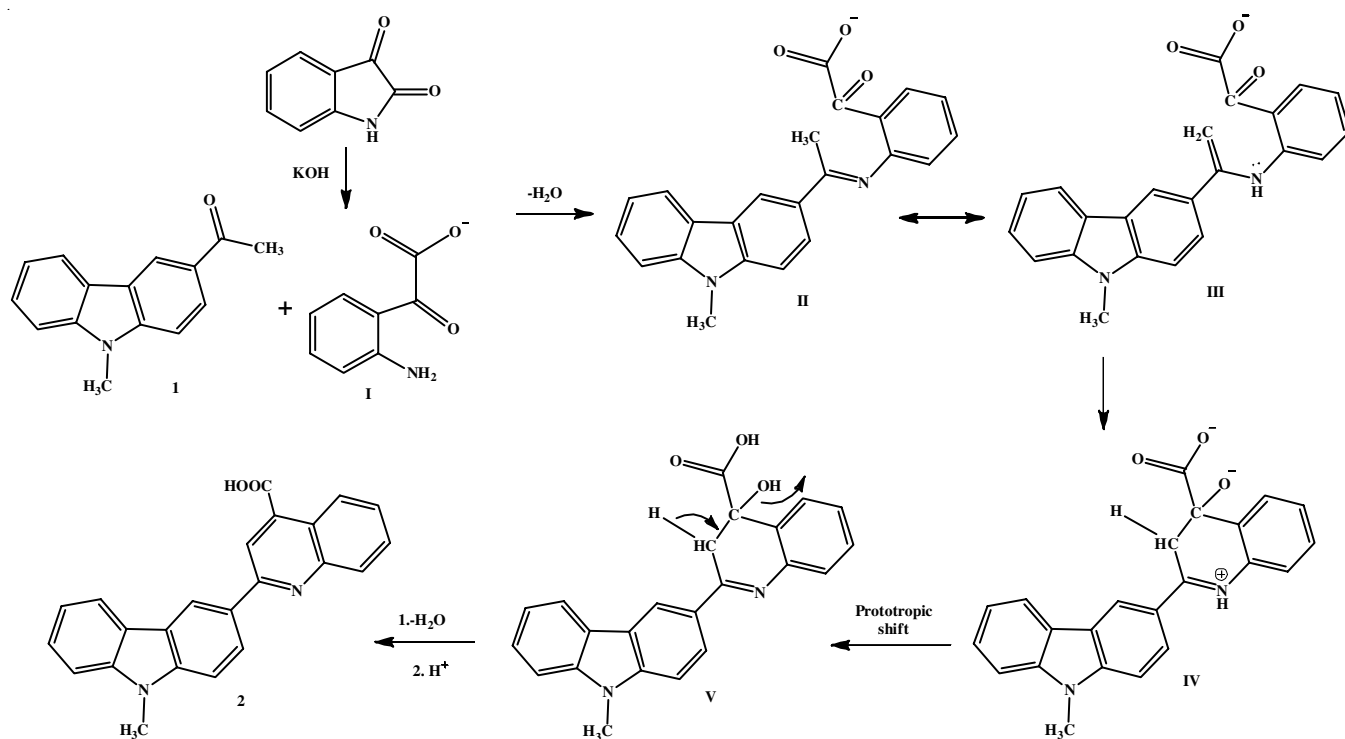
Protective layer characterization: A JEOL Scanning Electron Microscopy was utilized to investigate the surface characteristics of the mild steel samples in both inhibited along with uninhibited solutions.

RESULTS AND DISCUSSION

The synthon, 3-acetyl-*N*-methyl-carbazole (**1**) was synthesized according to the earlier reports [21-23]. In order to achieve the target compounds, the one of the way is to convert keto group into quinoline by means of well-known Pfitzinger reaction [24], in which a carbazole linked quinoline compound was synthesized by one step method. In brief, the reaction was accomplished by refluxing **3Ac-Cbz** (**1**) with isatin and NaOH in 20 mL of absolute ethanol for 24 h and the confirmation of completion was validated through TLC analysis. The obtained product was purified by sodium carbonate extraction followed by neutralization and then it was recrystallized from ethanol. The infrared spectrum of compound shows the presence of carboxylic acid group in **Cbz-QCA** (**2**). In $^1\text{H NMR}$, the singlet at δ 3.94 and 8.43 ppm belong to carbazole N-CH_3 and $\text{C}_4\text{-H}$, respectively and also the disappearance of $-\text{COCH}_3$ peak, which reveals the formation of product 3-(4-carboxyquinolin-2-yl)-9-methyl-9*H*-carbazole (**2**).

Mechanistically, compound **1** undergoes base catalyzed condensation with arylamino derivative (I) generated *in situ* from isatin to give an intermediate (II), which exists in equilibrium with the intermediate *N*-arylimine form (III). The intramolecular electrophilic substitution reaction assisted by lone pair electron on nitrogen at second position of carbazole intermediate, through the aryl carbonyl group afford the intermediate (IV). On ensuing the prototropic shift and dehydration, product 3-(4-carboxyquinolin-2-yl)-9-methyl-9*H*-carbazole (**2**) was yielded (**Scheme-II**).

Further, 4-chloroquinoline coupled carbazole product was obtained as a result of the reaction of **3Ac-Cbz** (**1**) and anthranilic acid in POCl_3 at $120 \text{ }^\circ\text{C}$ for 3 h. This product is then purified using column chromatography with an eluent ratio of 99:1% petroleum ether to ethyl acetate. It is possible to elucidate compound 3-(4-chloro-quinoline-2-yl)-9-methyl-9*H*-carbazole (**3**) due to the non-appearance of the carbonyl stretching frequency besides the existence of $-\text{C}=\text{N}$ stretching at 1581 cm^{-1} in the infrared spectrum. A further confirmation of the structure of **Cbz-CIQ** (**3**) is provided by the emergence of the $\text{N}_9\text{-CH}_3$ signal singlet at δ 3.94 and the twelve protons in the aromatic region



Scheme-II: Mechanistic pathway for the formation of Cbz-QCA (2)

at δ 7.33-8.95 and disappearance of acetyl methyl group in upfield in its ^1H NMR spectrum. ^{13}C NMR spectrum shows the presence of 22 carbons. The occurrence of the molecular ion peak at m/z 343 in the mass spectrum providing more evidence for the existence of 3-(4-chloroquinoline-2-yl)-9-methyl-9H-carbazole (3).

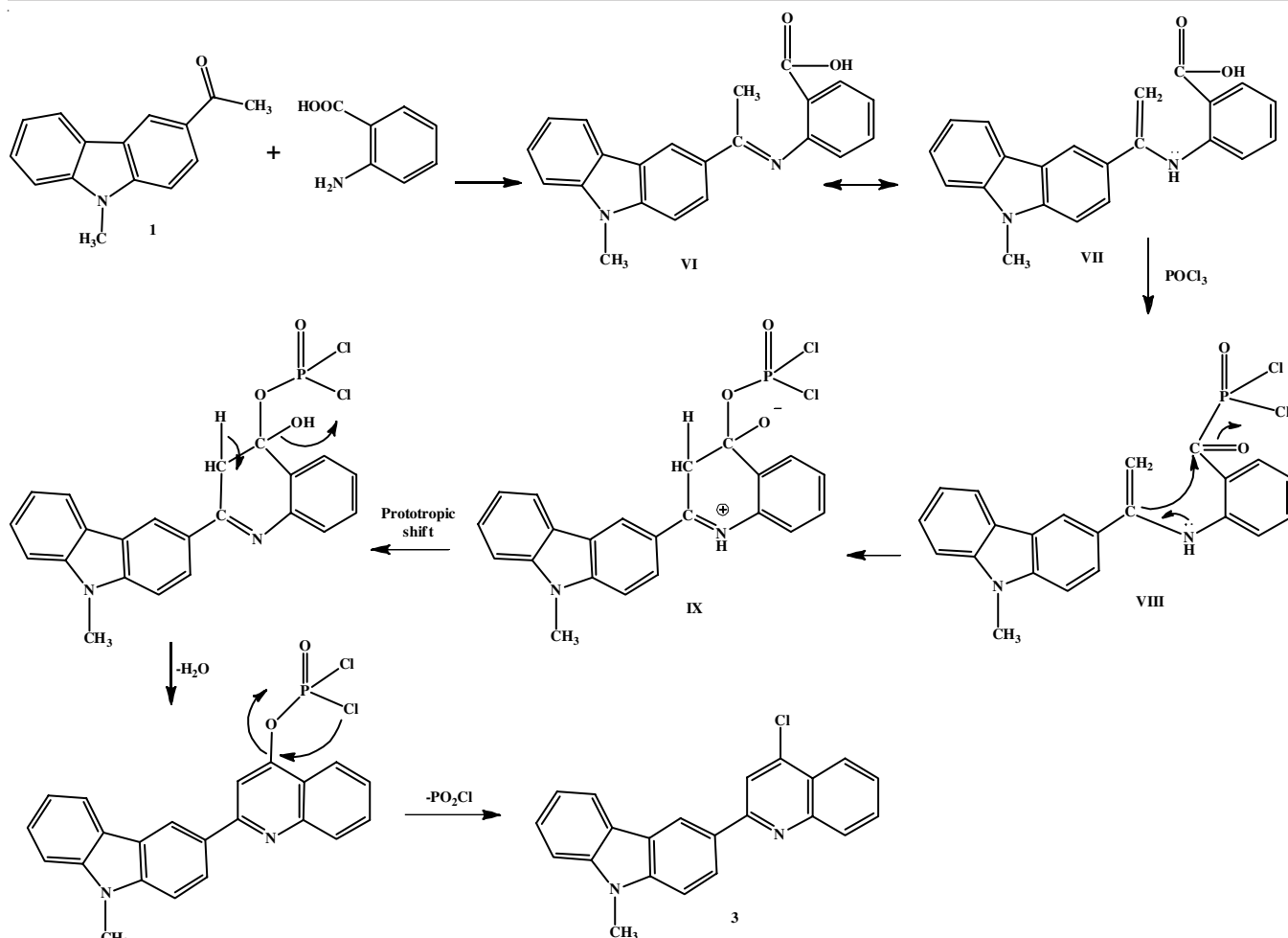
A plausible mechanism for the transformation of product 3 involves the reaction of compound 3-acetyl-*N*-methylcarbazole (1) catalyzed by phosphorous oxychloride acid. This leads condensation with anthranilic acid, resulting in the formation of an intermediate (VI) that exists in equilibrium with the *N*-aryl enamine form (VII). Subsequent treatment of the intermediate (VI) with excess POCl_3 produces a mixed anhydride intermediate (VIII). An intramolecular electrophilic substitution reaction at the second position of carbazole intermediate facilitated by the lone pair electron on nitrogen of the *N*-aryl moiety, leading to the formation of intermediate (IX). A prototropic shift, dehydrogenation and chlorination followed by PO_2Cl elimination, ultimately leads to the formation of the final product 3-(4-chloroquinoline)-2-yl-9-methyl-9H-carbazole (3) (Scheme-III).

Effect of inhibitor concentration: The non-electrochemical studies were carried out without/with chosen inhibitor concentrations in 1 M HCl at 308 K for approximately 2 h of exposure time in order to forecast the information about the kind of adsorption and the inhibitory capacity of the inhibitor. The results are presented in the Table-1. Compound 3Ac-Cbz was found to be exhibiting rise in inhibition efficiency upon enhancing the tested compounds concentration. From Table-1, it clearly demonstrates that when 3Ac-Cbz inhibitor concentration is increased and the protective effect also increased.

This is due to the interaction of carbazole aromatic ring electrons, with the lone pair of electrons from the N and O atoms and the electron density groups with the metal positively charged surface. In a similar way, the presence of prominent functional groups like methyl and acyl groups as well as benzene ring in 3Ac-Cbz are similarly limiting the mild steel corrosion. The protective effect increases proportionally with the enhancement of Cbz-QCA concentration. The IE% reaches a maximum of 89.14% at 1.25×10^{-3} M for Cbz-QCA.

TABLE-1
ASSESSMENT DATA OF NON ELECTROCHEMICAL ANALYSIS

Name of the inhibitor	Conc. (M)	Weight loss (g)	Inhibition efficiency (%)	Surface coverage (θ)	Corrosion rate (mpy)
3Ac-Cbz	0	0.6051	–	–	3.2846
	0.00025	0.1725	71.49	0.7149	0.9363
	0.00050	0.1481	75.52	0.7552	0.8039
	0.00075	0.1185	80.41	0.8041	0.6432
	0.00100	0.0692	88.56	0.8856	0.3756
	0.00125	0.0251	95.85	0.9585	0.1362
Cbz-QCA	0	0.6051	–	–	3.2846
	0.00025	0.1992	67.07	0.6707	1.0810
	0.00050	0.1689	72.08	0.7208	0.9168
	0.00075	0.1353	77.64	0.7764	0.7344
	0.00100	0.1103	81.77	0.8177	0.5987
	0.00125	0.0657	89.14	0.8914	0.3566
Cbz-CIQ	0	0.6051	–	–	3.2846
	0.00025	0.1944	67.87	0.6787	1.0552
	0.00050	0.1701	71.89	0.7189	0.9233
	0.00075	0.1582	73.86	0.7386	0.8587
	0.00100	0.1241	79.49	0.7949	0.6736
	0.00125	0.0916	84.86	0.8486	0.4972



Scheme-III: Mechanistic pathway for the formation of Cbz-ClQ (3)

Chetouani *et al.* [25,26] reported that the protective attributes of these compounds likely arise from the interaction between the π -electrons of the pyrazole rings and heteroatom with positively charged steel surface. Based on the evidence, it can be deduced that these compounds effectively inhibit steel corrosion in 1 M HCl solution. As depicted in Table-1, an increase on inhibitor concentration correlates with heightened inhibition efficacy and a reduction in the corrosion rate. At a concentration of 1.25×10^{-3} M, the inhibition efficiency is greater than 84%. The influence of inhibitor concentration on inhibition efficiency is minimal when Cbz-ClQ concentration is greater than 1.25×10^{-3} M. This demonstrates that mild steel corrosion by HCl is inhibited by the inclusion of an inhibitor within the solution and that the efficiency of corrosion inhibition depends on the amount of Cbz-ClQ presence. This pattern might be caused by the fact that as inhibitor concentration rises, both the amount of adsorption and the coverage of the inhibitor on the surface of mild steel also increases. As a result, the inhibitor adsorption coating effectively isolates the mild steel surface against the corrosive media.

Analysis of Tafel parameters: In Fig. 1, the anodic and cathodic Tafel curves for mild steel in 1M HCl solution are observed with and without 3Ac-Cbz, Cbz-QCA and Cbz-ClQ inhibitors. The Tafel parameters including E_{corr} (potential of

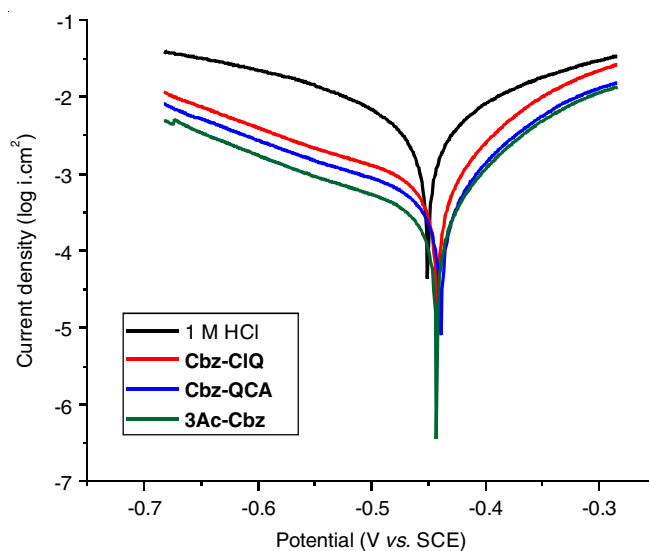


Fig. 1. Polarization plots of working electrode present in 1 M HCl containing maximal concentration of inhibitors

corrosion), I_{corr} (corrosion current density), b_a and b_c (anodic and cathodic Tafel slopes) were derived from Tafel plots and computed. The results (Table-2) show that the highest concentrations of the tested inhibitors generate considerable changes

TABLE-2
DATA OBTAINED FROM TAFEL CURVES OF MILD STEEL
IN 1 M HCl CONTAINING OPTIMUM CONCENTRATIONS
(0.00125 M) OF TESTED INHIBITORS

Test solutions	$-E_{\text{corr}}$ (mV)	j_{corr} ($\mu\text{A cm}^{-2}$)	$-b_c$ (mV/decade)	$-b_a$ (mV/decade)	IE (%)
HCl	451	5700	183.21	172.68	–
Cbz-ClQ	442	1041	226.25	104.45	81.73
Cbz-QCA	439	72.50	219.03	105.83	87.28
3Ac-Cbz	443	47.04	210.47	100.51	91.75

in the cathodic and, to a lesser extent, anodic sections of the polarization plots toward decreased current density when compared to the blank. On the other hand, the corrosion potential does not appear to have undergone any observable change. This pattern of behaviour indicates that all the inhibitors examined effectively mitigate the corrosion of mild steel in HCl. They function as mixed-type inhibitors, with prevailing cathodic impact. Additionally, the results demonstrated that the presence of optimal concentrations of the tested compounds do not significantly alter the cathodic Tafel slope compared to the blank.

The synthesized inhibitors, namely **3Ac-Cbz**, **Cbz-QCA** and **Cbz-ClQ** exhibit a significant impact on the cathodic and anodic processes (I_{corr}), leading to a reduction in the cathodic and anodic current densities as well as the corresponding corrosion current densities. It is suggested that the inhibitors interact with heteroatoms (N and O) and benzene ring electrons in **3Ac-Cbz**, **Cbz-QCA** and **Cbz-ClQ** molecules. Such interactions may create a protective layer on the mild steel surface, reducing the corrosive attack of the aggressive HCl solution and consequently increasing the inhibition efficiency with optimal concentrations of **3Ac-Cbz**, **Cbz-QCA** and **Cbz-ClQ**. Additionally, it was observed that the corrosion current density for mild steel in 1 M HCl significantly decreases in the presence of **3Ac-Cbz**, **Cbz-QCA** and **Cbz-ClQ** and this reduction was more pronounced with increasing inhibitor concentration. The increased obstruction in the portion of mild steel electrode surface resulting from adsorption leads to higher inhibitory efficiency [27] and with concentrations of 1.25×10^{-3} M, **3Ac-Cbz**, **Cbz-QCA** and **Cbz-ClQ** inhibitory efficiencies were exhibited at 91.75%, 87.28% and 81.73%, respectively. The study also demonstrates that all three inhibitors, **3Ac-Cbz**, **Cbz-QCA** and **Cbz-ClQ**, can effectively turn as noble corrosion inhibitors for mild steel in 1 M HCl environment. Among them, **3Ac-Cbz** promises a higher level performance compared to the other two inhibitors. The highest inhibition efficacy of **3Ac-Cbz**, **Cbz-QCA** and **Cbz-ClQ** is observed at their optimal concentrations. This observation implies that the hydrogen evolution reaction is controlled by activation and the presence of inhibitor does not modify the mechanism of the proton discharge reaction. Furthermore, the inhibition mechanism causes straightforward site blocking reactions. The inhibition efficiency (%IE) of the synthesized compounds has been computed and is provided in Table-2. Based on the data, it is evident that the optimum inhibition effect of the compounds follows the order **Cbz-ClQ** < **Cbz-QCA** < **3Ac-Cbz**. This sequence highlights the significance of molecular size, substituent groups in the inhibitor molecule and the variety of the functional adsorption atom in

the inhibition processes. The variation in inhibition efficiency through the optimum concentration of **3Ac-Cbz**, **Cbz-QCA** and **Cbz-ClQ** is depicted in Fig. 1. These plots all exhibit the characteristics of an adsorption isotherm, suggesting an adsorption mechanism for the action of the tested inhibitors on the mild steel surface. Furthermore, the sharp change in slope for all the curves indicates a mechanism involving monolayer adsorption over the mild steel surface.

Measurements of electrochemical impedance: EIS measurements were conducted to investigate the metal dissolution in the presence of inhibitors and gain a deeper understanding of the electrochemical processes occurring at the metal-solution interface. The experiments were involved in studying the corrosion of mild steel in a 1 mol/L solution with and without **3Ac-Cbz**, **Cbz-QCA** and **Cbz-ClQ** inhibitors. The obtained Nyquist plots (Fig. 2) deviate from the exact circles due to frequency depression [28]. Notably, the diameter of the capacitive loop is larger in the presence of **3Ac-Cbz**, **Cbz-QCA** and **Cbz-ClQ** compared to the blank solution. This observation provides evidence that the optimum concentration of the inhibitors enhances the impedance of mild steel. The increased impedance indicates a reduction in the metal dissolution, affirming the inhibitory effectiveness of the synthesized compounds against mild steel corrosion.

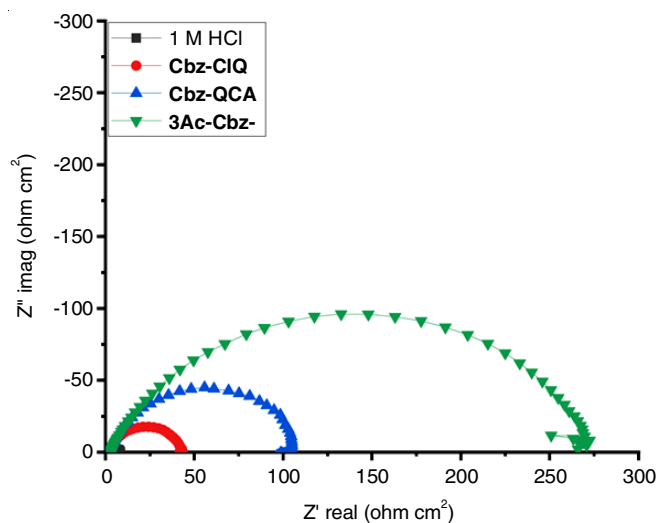


Fig. 2. Impedance curves for mild steel present in 1 M HCl containing optimum concentrations of tested inhibitors

The electrochemical data in Table-3 clearly indicated that at 1.25×10^{-3} M, the R_{ct} values were 127.3, 94.1 and 41.03 ohm cm^2 for **3Ac-Cbz**, **Cbz-QCA** and **Cbz-ClQ**, respectively. The increase in R_{ct} values in the inhibition efficiencies of 96.81, 95.69 and 90.12% for **3Ac-Cbz**, **Cbz-QCA** and **Cbz-ClQ**, respectively. The growth in R_{ct} values with increasing concentration indicates the development of an insulating protective coating at the metal contact, leading to the inhibition of corrosion. The increase in inhibition efficiency up to 1.25×10^{-3} M is associated with a decrease in C_{dl} values in response to the optimum inhibitory concentration. The decline in C_{dl} values can be attributed to a decrease in the local dielectric constant and an increase in the thickness of the electrical double layer.

TABLE-3
ELECTROCHEMICAL PARAMETERS FOR MILD STEEL
IN 1 M HCl SOLUTIONS CONTAINING OPTIMUM
CONCENTRATIONS (0.00125 M) OF TESTED INHIBITORS

Test solutions	R_s (Ω cm ²)	R_{ct} (Ω cm ²)	C_{dl} (F/cm ²)	IE (%)
HCl	2.921	4.05	2.51×10^{-2}	–
Cbz-CIQ	2.801	41.03	2.21×10^{-4}	90.12
Cbz-QCA	2.397	94.07	3.33×10^{-5}	95.69
3Ac-Cbz	2.781	127.29	2.51×10^{-5}	96.81

The clear decrease in C_{dl} values confirms the adsorption of the investigated inhibitor on the metal surfaces. The adsorption phenazine moiety on the metal surface and the reduction in the amount of metal dissolution contribute to the steady and slow replenishment of water molecules, which is reflected in the changing C_{dl} values.

Surface characteristics: The surface examination of the investigated metal surface, both in the presence and absence of **3Ac-Cbz**, **Cbz-QCA** and **Cbz-CIQ** inhibitors, was performed using scanning electron microscope (JOEL JSM 6390-Akikan Technology UK 5500 series). The SEM images of the pristine mild steel specimen reveal that immersion in 1 M HCl with the inhibitor (Fig. 3b-d) at a concentration of 0.0003 M illus-

trates the effect of **3Ac-Cbz**, **Cbz-QCA** and **Cbz-CIQ** inhibitors compared to an untreated mild steel surface (Fig. 3a), which appears extremely rough and damaged. The elements present in the **3Ac-Cbz**, **Cbz-QCA** and **Cbz-CIQ** inhibitors promote the formation of a protective layer on the mild steel surface, reducing the interaction between the metal and the acidic medium.

Comparison of corrosion inhibition efficiency: Table-4 provides a comparative analysis of weight loss, polarization and electrochemical measurements. The weight loss measurements were conducted for mild steel in 1 M HCl medium under two conditions *i.e.* in the presence and absence of different concentrations of **3Ac-Cbz**, **Cbz-QCA** and **Cbz-CIQ** inhibitor at 308 K.

Mechanism of corrosion inhibition: In uncontrolled acid solutions, the anions (Cl^-) from the aqueous HCl attach to the positively charged sites on the metal. In acidic environments, these anions can be protonated to form molecules due to lone pair electrons on the oxygen atom. However, in inhibited acid solutions, electrostatic repulsion prevents the protonated **3Ac-Cbz**, **Cbz-QCA** and **Cbz-CIQ** molecules from approaching the positively charged metal surface. Instead, the positively charged **3Ac-Cbz**, **Cbz-QCA** and **Cbz-CIQ** molecules from

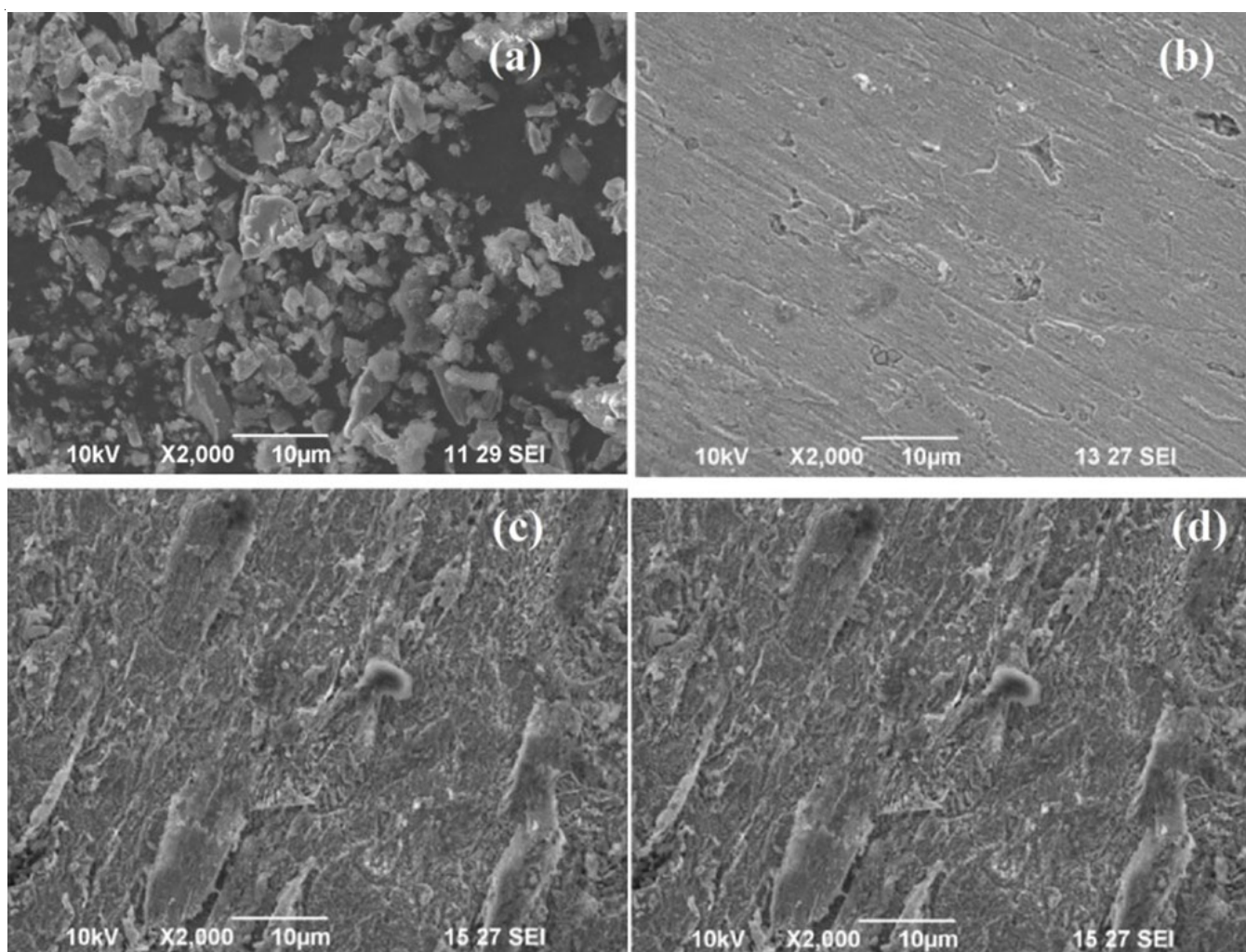


Fig. 3. SEM images of mild steel present in 1 M HCl (a), containing **3Ac-Cbz** (b), **Cbz-QCA** (c) and **Cbz-CIQ** inhibitor (d)

TABLE-4
COMPARISON OF INHIBITION EFFICIENCY (IE) OF **3Ac-Cbz**, **Cbz-QCA** AND **Cbz-CIQ** INHIBITOR FOR MS IN 1 M HCl (WEIGHT LOSS, POLARIZATION AND IMPEDANCE TECHNIQUES)

Synthetic inhibitors	Metal exposed	Best conc.	Corrosive media	Techniques (Highest % IE)			Ref.
				Mass loss	Tafel	Impedance	
N-((1 <i>H</i> -pyrrol-2-yl)methylene)nicotinamide	Mild steel	500 ppm	0.5 M HCl	80.60	83.80	83.00	[29]
N-((methyl-(phenyl)amino)methylene)nicotinamide	Mild steel	500 ppm	0.5 M HCl	86.30	86.6	85.40	[29]
N,N-bis(salicylidene)-2-hydroxy-1,3-propanediamine	Mild steel	0.005 M	2 M HCl	79.00	78.0	80.00	[30]
N-[(3,4-dimethoxyphenyl)methyleneamino]-4-hydroxy-benzamide	Mild steel	0.003 M	0.5 M H ₂ SO ₄	-	86.00	82.34	[31]
			0.5 M HCl	-	81.57	75.98	
1-[Morpholin-4-yl(thiophen-2-yl)methyl]thiourea	Mild steel	500 ppm	0.5 M HCl	-	86.27	83.81	[32]
2-Chloro 3-formyl quinoline	Mild steel	200 ppm	1 M HCl	88.22	85.03	85.34	[33]
3a,6a-Diphenyltetrahydro-1 <i>H</i> -imidazo[4,5- <i>c</i>][1,2,5]-thiadiazole-5(3 <i>H</i>)-thione 2,2-dioxide	Mild steel	120 μM	0.5 M H ₂ SO ₄	93.4	80.4	92.0	[34]
1-Ethyl-4-(2-(4-fluorobenzylidene)hydrazine-carbonyl)pyridin-1-ium iodide (IPyrC2H5)	Mild steel	5×10 ⁻⁵ M	1 M HCl	-	89.00	51.10	[35]
1-Butyl-4-(2-(4-fluorobenzylidene)hydrazinecarbonyl)-pyridin-1-ium iodide (IPyr-C4H9)	Mild steel	5×10 ⁻⁵ M	1 M HCl	-	92.40	63.10	[35]
5-(4-(Dimethylamino)phenyl)-3-phenyl-4,5-dihydro-1 <i>H</i> -pyrazole-1-carboxamide (DPC)	Mild steel	4×10 ⁻⁴ M	1 M HCl	-	63.95	82.19	[36]
3Ac-Cbz	Mild steel	1.25×10 ⁻³ M	1 M HCl	95.85	91.75	96.81	Present work
Cbz-QCA	Mild steel	1.25×10 ⁻³ M	1 M HCl	89.14	87.28	95.69	
Cbz-CIQ	Mild steel	1.25×10 ⁻³ M	1 M HCl	84.86	81.73	90.12	

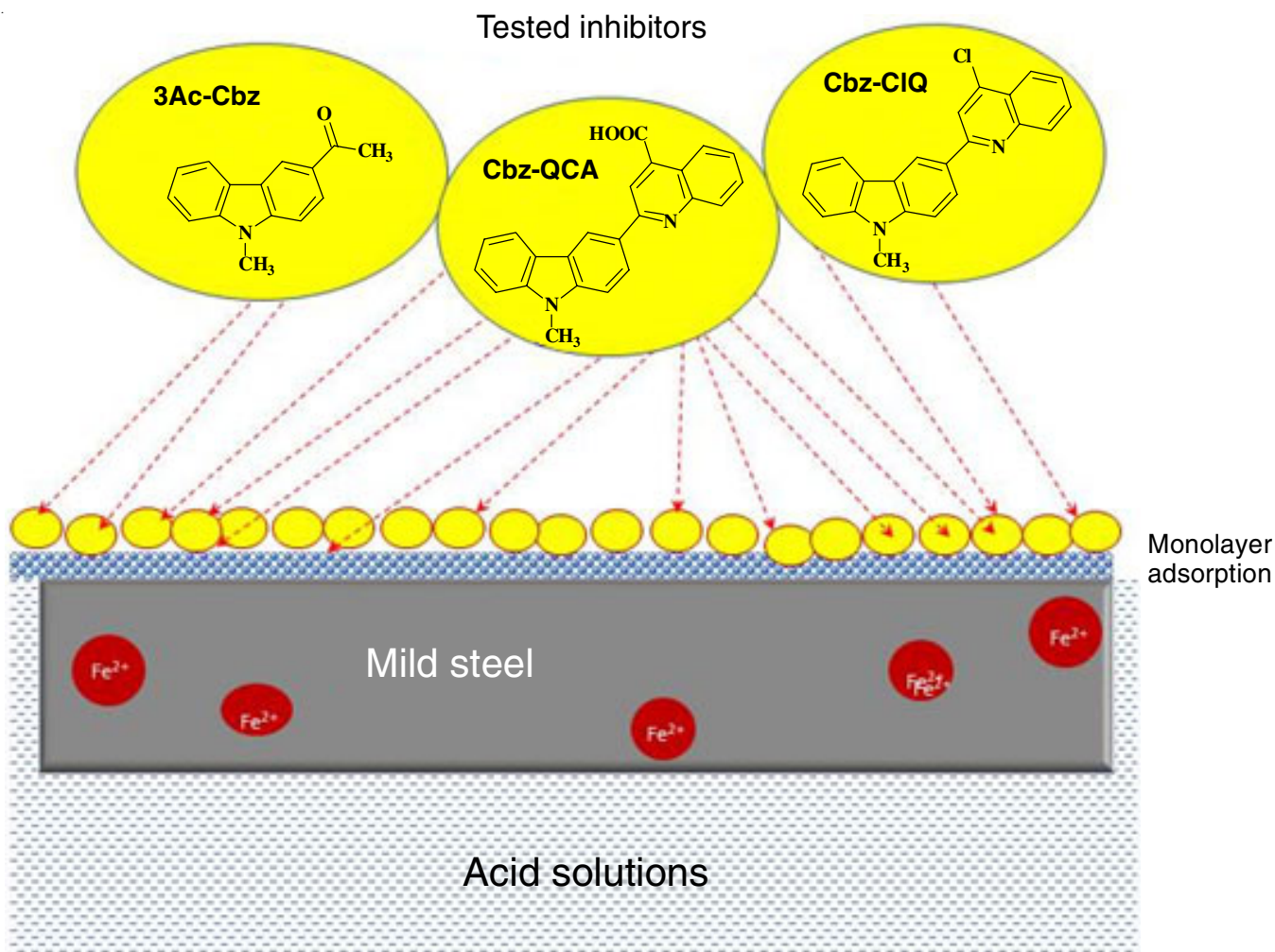


Fig. 4. Systematic representation of mechanism of inhibition of corrosion on mild steel

the solution can attach to the metal surface with the assistance of the anions, which act as bridge. On the working electrode surface, the adsorption sites that are not covered by anions are more likely to be occupied by non-protonated molecules. This results in an increase in the negative charge on the electrode surface due to electrostatic attraction with the Cl^- ions. However, the adsorption of protonated **3Ac-Cbz**, **Cbz-QCA** and **Cbz-CIQ** molecules counters this effect, reducing the negative charge on the electrode surface. Furthermore, the adsorption of protonated **3Ac-Cbz**, **Cbz-QCA** and **Cbz-CIQ** molecules inhibits the hydrogen evolution reaction at the cathodic site. The proposed schematic diagram (Fig. 4) illustrates the corrosion process of mild steel in HCl in both the absence and presence of **3Ac-Cbz**, **Cbz-QCA** and **Cbz-CIQ** inhibitors, taking into account the interactions between the anions, protonated molecules and the metal surface.

Conclusion

A facile one step synthesis of corresponding 3-(4-carboxyquinolin-2-yl)-9-methyl-9H-carbazole (**Cbz-QCA**) and 3-(4-chloroquinoline-2-yl)-9-methyl-9H-carbazole (**Cbz-CIQ**) by the reaction of 3-acetyl-9-methyl-9H-carbazole (**3Ac-Cbz**) as starting precursor with isatin and anthranilic acid, respectively, have been demonstrated and validated through spectral studies. Detailed discussions on the potential mechanisms for the formation of the final products have been provided. The synthesized compounds have shown the positive acidic medium corrosion inhibition characteristics. As the concentration of inhibitor increases, the effectiveness of the inhibitor increases, as demonstrated that the investigated molecules spontaneously adsorb in the corrosive medium on the metal surface. The hetero atoms, N- and O-atoms and π -electron centers of the dibenzopyrrole rings act as the main reactive sites in **3Ac-Cbz**, enabling strong interactions with Fe and consequently, binding to the metal surfaces, according to the weight loss calculations supported the aforementioned experimental findings. The inhibition efficiency of **Cbz-QCA** increases with the concentration to attain a maximum value 89.14% at 308 K. The inhibition efficiency of **Cbz-QCA** decreases with the studied temperature. The inhibition efficiency of **Cbz-CIQ** increases with the increase of its concentration but it significantly decreases with an decrease in concentration at 1.25×10^{-3} to 2.5×10^{-4} M.

ACKNOWLEDGEMENTS

One of the authors, V. Panneerselvi, acknowledges the award of Savitribai Jyotirao Phule Single Girl Child Fellowship-Junior Research Fellowship by University Grant Commission, New Delhi, India.

CONFLICT OF INTEREST

The authors declare that there is no conflict of interests regarding the publication of this article.

REFERENCES

- Q. Ma, J. Tian, J. Yang, A. Wang, T. Ji, Y. Wang and Y. Su, *Fitoterapia*, **87**, 1 (2013); <https://doi.org/10.1016/j.fitote.2013.03.003>
- V. Mani, K. Ramasamy, A. Ahmad, M. Parle, S.A.A. Shah and A.B.A. Majeed, *Food Chem Toxicol.*, **50**, 1036 (2012); <https://doi.org/10.1016/j.fct.2011.11.037>
- V. Panneerselvi, K. Shankar and K. Prabakaran, *J. Heterocycl. Chem.*, **60**, 2081 (2023); <https://doi.org/10.1002/jhet.4740>
- J. Aslam, R. Aslam, S.H. Alrefaee, M. Mobin, A. Aslam, M. Parveen and C.M. Hussain, *Arab. J. Chem.*, **13**, 7744 (2020); <https://doi.org/10.1016/j.arabjc.2020.09.008>
- D.L. Crossley, C.D. Gabbutt, B.M. Heron, P. Kay and M. Mogstad, *Dyes Pigment*, **95**, 62 (2012); <https://doi.org/10.1016/j.dyepig.2012.03.031>
- J. Wang, L. An, J. Wang, J. Gu, J. Sun and X. Wang, *Adv. Colloid Interf. Sci.*, **321**, 103031 (2023); <https://doi.org/10.1016/j.cis.2023.103031>
- M.A. Quraishi, D.S. Chauhan and V.S. Saji, *J. Mol. Liq.*, **341**, 117265 (2021); <https://doi.org/10.1016/j.molliq.2021.117265>
- G. Senthilkumar, C. Umarani and A. Ramachandran, *J. Indian Chem. Soc.*, **98**, 100079 (2021); <https://doi.org/10.1016/j.jics.2021.100079>
- H. Wang, X. Wang, H. Wang, L. Wang, A. Liu, *J. Mol. Model.*, **13**, 147 (2007); <https://doi.org/10.1007/s00894-006-0135-x>
- L.O. Olasunkanmi, M.M. Kabanda and E.E. Ebenso, *Physica E Low Dimens. Syst. Nanostruct.*, **76**, 109 (2016); <https://doi.org/10.1016/j.physe.2015.10.005>
- J. Saranya, P. Sounthari, K. Parameswari and S. Chitra, *Measurement*, **77**, 175 (2016); <https://doi.org/10.1016/j.measurement.2015.09.008>
- J.A. Nasser and M.A. Sathiq, *Int. J. Eng. Sci. Technol.*, **21**, 6417 (2010).
- G. Gunasekaran and L.R. Chauhan, *Electrochim. Acta*, **49**, 4387 (2004); <https://doi.org/10.1016/j.electacta.2004.04.030>
- M. Bouklah, A. Attayibat, B. Hammouti, A. Ramdani, S. Radi and M. Benkaddour, *Appl. Surf. Sci.*, **240**, 341 (2005); <https://doi.org/10.1016/j.apsusc.2004.07.001>
- A. Aouniti, B. Hammouti, S. Kertit and M. Brighli, *Bull. Electrochem.*, **14**, 193 (1998).
- G. Subramaniam, K. Balasubramanian and P. Sridhar, *Corros. Sci.*, **30**, 1019 (1990); [https://doi.org/10.1016/0010-938X\(90\)90209-N](https://doi.org/10.1016/0010-938X(90)90209-N)
- Y. Xiao-Ci, Z. Hong, L. Ming-Dao, R. Hong-Xuan and Y. Lu-An, *Corros. Sci.*, **42**, 645 (2000); [https://doi.org/10.1016/S0010-938X\(99\)00091-8](https://doi.org/10.1016/S0010-938X(99)00091-8)
- M. Lashkari and M.R. Arshadi, *Chem. Phys.*, **299**, 131 (2004); <https://doi.org/10.1016/j.chemphys.2003.12.019>
- K. Tebbji, I. Bouabdellah, A. Aouniti, B. Hammouti, H. Oudda and M.A. Ramdani, *Mater. Lett.*, **61**, 799 (2007); <https://doi.org/10.1016/j.matlet.2006.05.063>
- A. Chetouani, M. Daoudi, B. Hammouti, T. Ben Hadda and M. Benkaddour, *Corros. Sci.*, **48**, 2987 (2006); <https://doi.org/10.1016/j.corsci.2005.10.011>
- Z. Shufen, Z. Danhong and Y. Jinzong, *Dyes Pigm.*, **27**, 287 (1994); [https://doi.org/10.1016/0143-7208\(94\)00054-6](https://doi.org/10.1016/0143-7208(94)00054-6)
- V.K.R. Avula, S. Vallela, J.S. Anireddy and N. RajuChamarthi, *J. Heterocycl. Chem.*, **54**, 2471 (2017); <https://doi.org/10.1002/jhet.2847>
- T. Bzeih, T. Naret, A. Hachem, N. Jaber, A. Khalaf, J. Bignon, J.D. Brion, M. Alami and A. Hamze, *Chem. Commun.*, **52**, 13027 (2016); <https://doi.org/10.1039/C6CC07666A>
- J.N. Sangshetti, A.S. Zambare, I. Gonjari and D.B. Shinde, *Mini. Rev. Org. Chem.*, **11**, 225 (2014); <https://doi.org/10.2174/1570193X113106660020>
- L. Herrag, A. Chetouani, S. Elkadiri, B. Hammouti and A. Aouniti, *Portug. Electrochim. Acta*, **26**, 211 (2008).
- A. Chetouani, A. Aouniti, B. Hammouti, N. Benchat, T. Benhadda and S. Kertit, *Corros. Sci.*, **45**, 1675 (2003); [https://doi.org/10.1016/S0010-938X\(03\)00018-0](https://doi.org/10.1016/S0010-938X(03)00018-0)
- A. Sehmi, H.B. Ouici, A. Guendouzi, M. Ferhat, O. Benali and F. Boudjellal, *J. Electrochem. Soc.*, **167**, 155508 (2020); <https://doi.org/10.1149/1945-7111/abab25>

28. W. Xu, E.H. Han and Z. Wang, *J. Mater. Sci. Technol.*, **35**, 64 (2019); <https://doi.org/10.1016/j.jmst.2018.09.001>
29. M.P. Chakravarthy, K.N. Mohana and C.B. Pradeep Kumar, *Int. J. Ind. Chem.*, **5**, 19 (2014); <https://doi.org/10.1007/s40090-014-0019-3>
30. K.C. Emregul, A.A. Akay and O. Atakol, *Mater. Chem. Phys.*, **93**, 325 (2005); <https://doi.org/10.1016/j.matchemphys.2005.03.008>
31. K. Muthamma, P. Kumari, M. Lavanya and S.A. Rao, *J. Bio Tribo Corros.*, **7**, 10 (2021); <https://doi.org/10.1007/s40735-020-00439-7>
32. D.K. Lavanya, F.V. Priya and D.P. Vijaya, *J. Fail. Anal. Preven.*, **20**, 494 (2020); <https://doi.org/10.1007/s11668-020-00850-9>
33. B.M. Prasanna, B.M. Praveen, N. Hebbar, T.V. Venkatesha and H.C. Tandon, *Int. J. Ind. Chem.*, **7**, 9 (2020); <https://doi.org/10.1007/s40090-015-0064-6>
34. M.J. Banera, J.A. Caram, C.A. Gervasi and M.V. Mirifico, *J. Appl. Electrochem.*, **44**, 1337 (2014); <https://doi.org/10.1007/s10800-014-0729-4>
35. F. EL-Hajjaji, E. Ech-chihbi, N. Rezki, F. Benhiba, M. Taleb, D.S. Chauhan and M.A. Quraishi, *J. Mol. Liq.*, **314**, 113737 (2020); <https://doi.org/10.1016/j.molliq.2020.113737>
36. A. Sehmi, H.B. Ouici, A. Guendouzi, M. Ferhat, O. Benali and F. Boudjellal, *J. Electrochem. Soc.*, **167**, 155508 (2020); <https://doi.org/10.1149/1945-7111/abab25>